Structure of Cyclodextrin Glycosyltransferase Complexed with a Maltononaose Inhibitor at 2.6 Å Resolution. Implications for Product Specificity

ARTICLE *in* BIOCHEMISTRY · MAY 1996

Impact Factor: 3.02 · DOI: 10.1021/bi952339h · Source: OAI

Structure of Cyclodextrin Glycosyltransferase Complexed with a Maltononaose Inhibitor at 2.6 Å Resolution. Implications for Product Specificity[†,‡]

Boris Strokopytov,[§] Ronald M. A. Knegtel,[§] Dirk Penninga,[||] Henriëtte J. Rozeboom,[§] Kor H. Kalk,[§] Lubbert Dijkhuizen,[||] and Bauke W. Dijkstra*[,§]

BIOSON Research Institute and Laboratory of Biophysical Chemistry, Groningen Biomolecular Sciences and Biotechnology Institute, University of Groningen, Nijenborgh 4, 9747 AG Groningen, The Netherlands, and Department of Microbiology, Groningen Biomolecular Sciences and Biotechnology Institute, University of Groningen, Kerklaan 30, 9751 NN Haren, The Netherlands

Received September 29, 1995; Revised Manuscript Received December 22, 1995[⊗]

ABSTRACT: Crystals of the Y195F mutant of cyclodextrin glycosyltransferase from *Bacillus circulans* strain 251 were subjected to a double soaking procedure, in which they were first soaked in a solution containing the inhibitor acarbose and subsequently in a solution containing maltohexaose. The refined structure of the resulting protein−carbohydrate complex has final crystallographic and free *R*-factors for data in the 8−2.6 Å resolution range of 15.0% and 21.5%, respectively, and reveals that a new inhibitor, composed of nine saccharide residues, is bound in the active site. The first four residues correspond to acarbose and occupy the same subsites near the catalytic residues as observed in the previously reported acarbose−enzyme complex [Strokopytov et al. (1995) *Biochemistry 34,* 2234−2240]. An oligosaccharide consisting of five glucose residues has been coupled to the nonreducing end of acarbose. At the fifth residue the polysaccharide chain makes a sharp turn, allowing it to interact with residues Tyr89, Phe195, and Asn193 and a flexible loop formed by residues 145−148. On the basis of the refined model of the complex an explanation is given for the product specificity of CGTases.

Enzymes such as amylases and cyclodextrin glycosyltransferases (CGTases)[1] degrade starch to smaller oligosaccharides by hydrolyzing the α-D-(1→4) linkages between glucose residues present in starch. In the case of CGTases, in addition a cyclization reaction is catalyzed, yielding mixtures of cyclic oligosaccharides, referred to as α-, *β*-, or *γ*-cyclodextrins (CDs) (consisting of six, seven, or eight glucoses, respectively). CGTases are characterized as α-, *β*-, or *γ*-CTGases, depending on the major product of the cyclization reaction. Besides having similar catalytic site residues, amylases and CGTases contain carbohydrate binding domains that are distant from the active site (Svensson et al., 1989). These sugar binding domains have been implicated in attaching the enzyme to raw starch granules and in guiding the amylose chain into the active site (Buisson et al., 1987; Svensson et al., 1989; Lawson et al., 1994).

The structural studies on amylases and CGTases that have been reported until now have provided insight into the overall fold of these enzymes and their catalytic mechanism. We study the CGTase from *Bacillus circulans* strain 251. Recently, we reported the three-dimensional structure of this enzyme at 2.0 Å resolution (Lawson et al., 1994) and its complexes with the inhibitor acarbose (Strokopytov et al., 1995) and natural substrates such as maltotetraose and α-cyclodextrin (Knegtel et al., 1995). The enzyme consists of five domains, labeled A through E, of which the A domain folds into a $(\beta/\alpha)_8$ barrel while the other domains consist mainly of *β*-sheets and loop regions. A similar fold was reported for the CGTase from *B. circulans* strain 8 (Klein & Schulz, 1991). Amylases have a three-dimensional structure which is similar to the A, B, and C domains of CGTase, but they lack the additional D and E domains that are unique for CGTases. In the case of the CGTase from *B. circulans* strain 251, the E domain was found to bind two maltoses at two putative raw starch binding sites. A third maltose was observed to bind at the C domain (Lawson et al., 1994).

On the basis of the structures of complexes between CGTase and acarbose or maltotetraose, distinct catalytic roles could be assigned to the active site residues Asp229, Glu257, and Asp328 (Strokopytov et al., 1995; Knegtel et al., 1995). The carboxylic group of Glu257 is at hydrogen-bonding distance from the glycosidic oxygen of the scissile bond between the 1 and −1 glucoses of the substrate (cf. Figures 1 and 5 for the nomenclature) and acts as the proton donor in the hydrolytic reaction. Asp229 serves as the general base or nucleophile and stabilizes the putative oxocarbonium intermediate formed after cleavage of the substrate. In addition, it could distort the conformation of the 1 sugar prior to catalysis by hydrogen bonding to its C6 hydroxyl group. Asp328 is involved in substrate binding and elevates the pK_a

[†] This work was financially supported by the Nederlandse Programma Commissie voor Biotechnologie (PCB) of the Ministry of Economic Affairs and the Groningen Biomolecular Sciences and Biotechnology Institute (GBB).

[‡] Atomic coordinates for the complex have been deposited with the Brookhaven Protein Data Bank (file name 1DIJ).

* Author to whom all correspondence should be addressed [fax, (++31) 50 363 48 00; e-mail, bauke@chem.rug.nl].

[§] BIOSON Research Institute and Laboratory of Biophysical Chemistry.

[||] Department of Microbiology.

[⊗] Abstract published in *Advance ACS Abstracts,* March 15, 1996.

[1] Abbreviations: CGTase, cyclodextrin glycosyltransferase; MPD, 2-methyl-2,4-pentanediol; Hepes, *N*-(2-hydroxyethyl)piperazine-*N*′-2-ethanesulfonic acid; rms, root mean square; α-, *β*-, and *γ*-CD, α-, *β*-, and *γ*-cyclodextrin; G3, maltotriose; G5, maltopentaose; G6, maltohexaose; G7, maltoheptaose; G9, maltononaose; CAPS, 3-(cyclohexylamino)-1-propanesulfonic acid.

0006-2960/96/0435-4241$12.00/0

of Glu257 through a direct hydrogen bond that is observed in the uncomplexed CGTase structure. A similar picture of substrate binding and catalysis was derived from structural studies on amylases (Buisson et al., 1987; Larson et al., 1994; Qian et al., 1993, 1994).

Although the use of relatively small inhibitors has provided detailed insight into the catalytic mechanisms of amylases and CGTases, the question of how starch-degrading enzymes bind longer amylose chains has remained unresolved. In addition, the exact role of the raw starch binding domains in substrate binding and catalysis is still unclear. In the case of CGTases, the oligosaccharide that is cleaved off from the starch chain must remain bound to the enzyme, and its nonreducing end must fold back into the active site for cyclization to occur. Assuming that the largest CDs produced by the enzyme are γ-CDs, this would require the presence of at least eight glucose binding sites starting from the cleavage site. Indeed, kinetic studies of the α-CGTase from *Klebsiella pneumoniae* strain M 5 a1 and the β-CGTase from *B. circulans* strain 8 showed that the active sites of both enzymes contain nine subsites with cleavage taking place after the third and second binding site, respectively (Bender, 1990). A number of modeling studies aimed at predicting the binding mode of linear substrates to CGTase have been reported, based on the crystal structures of unliganded CGTase (Lawson et al., 1994; Mattsson et al., 1995; Nakamura et al., 1994). These studies have implicated various residues or regions on the protein surface in ligand binding, without providing much detail on the exact enzyme−substrate interactions. Precise knowledge of the nature of the substrate binding sites would increase our understanding of the factors determining the specificity of CGTases for producing different ratios of α-, β-, and γ-CDs. In order to resolve these issues, structural information is required on the interaction between starch-degrading enzymes and longer substrates, which bind to sites distant from the active site. Such an approach has been successful in providing more insight into the structural basis of substrate binding by lysozyme (Cheetham et al., 1992; Maenaka et al., 1995; Strynadka & James, 1991). In this paper, we present the three-dimensional structure of the CGTase from *B. circulans* strain 251 complexed simultaneously with a maltononaose inhibitor, maltose, maltotriose, and maltopentaose and demonstrate how protein−substrate interactions remote from the catalytic site can determine product specificity. The present studies were carried out with a Y195F mutant (Penninga et al., 1995) because of the ample availability of good quality crystals. This mutant has 60% of the cyclization and 40% of the coupling activity of the wild-type enzyme but similar disproportionation and saccharifying activities. From this it has been proposed that the residue at position 195 has a (as yet unknown) function in the interaction with cyclic substrates and products (Penninga et al., 1995).

MATERIALS AND METHODS

Purification of the Y195F CGTase mutant was performed according to Penninga et al. (1995). Crystals suitable for X-ray diffraction were grown in the course of 3−4 weeks under conditions similar to those used for the wild-type CGTase (Lawson et al., 1990). They belong to the same orthorhombic space group $P2_12_12_1$ and have cell dimensions similar to those of the wild-type enzyme crystals. After crystallization the crystals were transferred to a stabilizing mother liquor containing 60% (v/v) MPD (2-methyl-2,4-pentanediol) and 100 mM Na Hepes buffer [*N*-(2-hydroxyethyl)piperazine-*N*′-2-ethanesulfonic acid], at pH 7.55, containing 0.5% (w/v) maltose.

Table 1: Data Collection Statistics and Quality of the Final Model[a]

cell dimensions ($P2_12_12_1$)	
a (Å)	120.0
b (Å)	111.3
c (Å)	68.0
resolution range (Å)	28.0−2.6
total no. of observations	79898
no. of discarded observations	4004
no. of unique reflections	27013
R_{merge}	0.064
R_{merge} (2.64−2.60 Å)	0.132
completeness of data (%)	94.1
completeness (%) (2.64−2.60 Å)	71.7
refinement resolution range (Å)	8.0−2.6
no. of protein non-hydrogen atoms	5263
no. of calcium atoms	2
no. of carbohydrate non-hydrogen atoms	212
no. of solvent sites	126
average *B*-factor (Å^2)	13.6
final *R*-factor/*R*-free (%)	15.0/21.5
rms deviations from ideality for	
bond lengths (Å)	0.013
bond angles (deg)	1.4
torsion angles (deg)	17.9
trigonal planes (Å)	0.012
planar groups (Å)	0.013
van der Waals contacts (Å)	0.018
rms difference in *B* for neighboring atoms (Å^2)	2.8

[a] R_{merge} is defined as $R_{merge} = (\Sigma\Sigma|I_j(hkl) - \langle I(hkl)\rangle|)/(\Sigma\Sigma\langle I(hkl)\rangle)$, and the crystallographic *R*-factor is defined as $R = \Sigma||F_o| - |F_c||/\Sigma|F_o|$. Free *R*-factors were calculated using 10% of the unique reflections. Observations were discarded when they deviated by more than 2.5 times the standard deviation from the average intensity.

The active site of CGTase is not blocked in the crystal by symmetry-related molecules and can therefore easily be accessed by ligands. This allowed us previously to obtain enzyme−inhibitor complexes by soaking native enzyme crystals in solutions containing the inhibitor acarbose (Strokopytov et al., 1995). For the work described here a double soaking technique was applied in an attempt to observe binding of longer carbohydrates to the enzyme. Protein−inhibitor complexes were prepared by soaking crystals of the Y195F mutant for 1 week in a buffer solution containing 60% MPD (v/v), 0.1 M CAPS [3-(cyclohexylamino)-1-propanesulfonic acid] buffer, pH 9.8, and 0.25% (w/v) acarbose. Subsequently, the buffer was replaced by the same mother liquor containing 0.5% (w/v) maltohexaose (G6) at pH 9.8 instead of acarbose, and soaking was continued for an additional week. During soaking with G6 small cracks appeared at the crystal surface on the second and third days of soaking which gradually disappeared during further soaking.

After a total soaking time of 2 weeks in the acarbose and G6 solutions, the crystal was mounted in a capillary and X-ray data were collected at room temperature on an Enraf Nonius FAST area detector system, with an Elliot GX21 rotating anode generator as the X-ray source. Data collection and processing were performed with MADNES (Messerschmidt & Pflugrath, 1987) with profile fitting of the intensities according to Kabsch (1988). A summary of data collection statistics is given in Table 1. Only the length of

the *c*-axis of the double soaked crystal (68.0 Å) deviates significantly from the corresponding value for uncomplexed Y195F mutant crystals (66.3 Å) (Penninga et al., 1995).

Crystallographic refinement of the crystal structure was performed with the TNT package (Tronrud et al., 1987) using the 2.0 Å structure of native CGTase as the starting model. The model contained all 686 residues, two calcium ions, and three maltose molecules. Water molecules with *B*-values larger than 40 Å^2 and all active site waters had been removed from the starting model to allow for an unambiguous detection of potential carbohydrate density in the active site cleft. Residue Tyr195 in the native protein was replaced by a Phe prior to rigid body refinement. Manual adjustments and fitting of carbohydrate density were performed with FRODO (Jones, 1978) running on an Evans and Sutherland PS390 computer graphics station or O (Jones et al., 1991) running on Silicon Graphics workstations.

A rigid body refinement with TNT rotated the starting structure over 1.3° and shifted it by about −0.47, 0.25, and 0.34 Å along the *x*-, *y*-, and *z*-coordinate axes, respectively. This decreased the *R*-value from 47% to 25% in the 8.0−2.6 Å resolution range. A σ_a-weighted difference Fourier map with $(2mF_o - DF_c)\exp(i\alpha_{calc})$ coefficients (Read, 1986) was calculated and showed continuous density in the active site cleft, corresponding to nine fully occupied subsites. The ligand electron density was of such quality that the glucose C6-hydroxyl groups could easily be identified. The shape of the density suggested that subsites −2 to 2 in the active site were occupied by an acarbose molecule which had become covalently linked at the nonreducing end via an α-D-(1,4) linkage to a maltopentaose molecule occupying five additional subsites. The possibility of fitting two separate carbohydrate molecules in the observed density was checked and rejected. In addition, inspection of the electron density at the maltose binding sites located in the E domain allowed us to place an additional maltopentaose (G5) near Tyr633 (the second maltose binding site) and a maltotriose (G3) molecule in the vicinity of Trp616 and Trp662, which constitute the first maltose binding site. At the third maltose binding site (near Tyr413), which is involved in crystal packing contacts, only density corresponding to a maltose molecule was observed. All oligosaccharide models were introduced immediately after the rigid body refinement, and the resulting model was subjected to all-parameter refinement. Tight restraints were applied on bond lengths, bond angles, *B*-factor correlation between bonded atoms, planarity of groups, and trigonal centers during least-squares refinement but not on chiral centers or torsion angles. Ideal bond lengths and angles were taken from Engh and Huber (1991). Free *R*-factors (Brünger, 1993) were calculated using 10% of the structure factors during the last 30 cycles of the refinement. In addition, the final structure was subjected to a 3000−300 K simulated annealing run with X-PLOR (Brünger et al., 1990) as an alternative method to determine the final free *R*-factor. Additional water molecules were added if their density in $(m|F_o| - D|F_c|)$ electron density maps exceeded 3.5σ and at least one hydrogen bond was formed with the protein, carbohydrates, or existing water molecules.

The refinement was halted when no further improvement was observed in the *R*-factors. Refinement statistics are listed in Table 1. The quality of the final model was checked with the PROCHECK package (Laskowski et al., 1993). Coordinates of the model of CGTase complexed with carbohydrates have been deposited with the Protein Data Bank (Bernstein et al., 1977) (entry code 1DIJ).

RESULTS

Structure Refinement. The final model of CGTase complexed with a maltononaose inhibitor and substrates has excellent stereochemistry, a crystallographic *R*-factor of 15.0%, and a free *R*-factor of 21.5% as is shown in Table 1. The free *R*-factor obtained with the program X-PLOR is 21.7%. Its Ramachandran plot is virtually identical to that of the native CGTase protein (Lawson et al., 1994). The $(2F_o - F_c)$ electron density of the carbohydrate ligands is shown in Figures 1 and 2. It is clear that the sugars of the maltononaose inhibitor are well-defined in the electron density. Although at maltose binding site 1 clearly only electron density is observed for a maltotriose, the electron density at maltose binding site 2 does not exclude that actually an oligosaccharide larger than maltopentaose is bound of which the outer sugars are not observed due to increased flexibility. All protein residues that directly contact the bound maltononaose are well-defined in the electron density maps. Most residues found to be disordered in the native structure remain disordered in the protein−inhibitor complex. A number of residues in the loop 145−148, however, have slightly better electron densities.

Comparison of the native and complexed CGTase structure yields a root-mean-square coordinate difference of about 0.26 Å for all C_α atoms (0.27 and 0.40 Å for main chain and all atoms, respectively), which is comparable to the mean coordinate error of 0.2 Å as estimated from a σ_a plot (Read, 1986). The largest changes in the protein backbone conformation are in the order of 0.8−0.9 Å and occur at flexible loops near residues 140−155 and 160−200, which interact with the inhibitor, as well as the maltose binding sites in the E domain where maltotriose and maltopentaose are bound. The structural changes induced by binding of the ligand to CGTase are depicted in Figure 3, where the C_α traces of the native CGTase structure (Lawson et al., 1994) and that of the complex with the maltononaose inhibitor are compared after superpositioning.

Binding of the Maltononaose Inhibitor. The final model of the enzyme−inhibitor complex allows for a detailed analysis of the interactions between a long carbohydrate chain and the active site of CGTase. Since the nomenclature employed in the description of the CGTase−acarbose complex (Strokopytov et al., 1995), which used labels A through D for the different sugar residues, is not conveniently applicable to a maltononaose, we use a nomenclature similar to that introduced by Klein et al. (1992) in which the scissile bond between acarbose residues B and C is taken as the new starting point for numbering the sugars of the inhibitor. In the new nomenclature residues A, B, C, and D in acarbose are numbered 2, 1, −1, and −2 (cf. Figures 1 and 5) to indicate whether they are located in the amylose chain before (negative numbers increasing toward the reducing end) or after (positive numbers increasing toward the nonreducing end) the point of cleavage. The five glucose units following residue 2 (the former sugar residue A) of acarbose are thus numbered 3−7.

The first four subsites, labeled −2 through 2, are occupied by sugar residues of acarbose, in an identical way as was

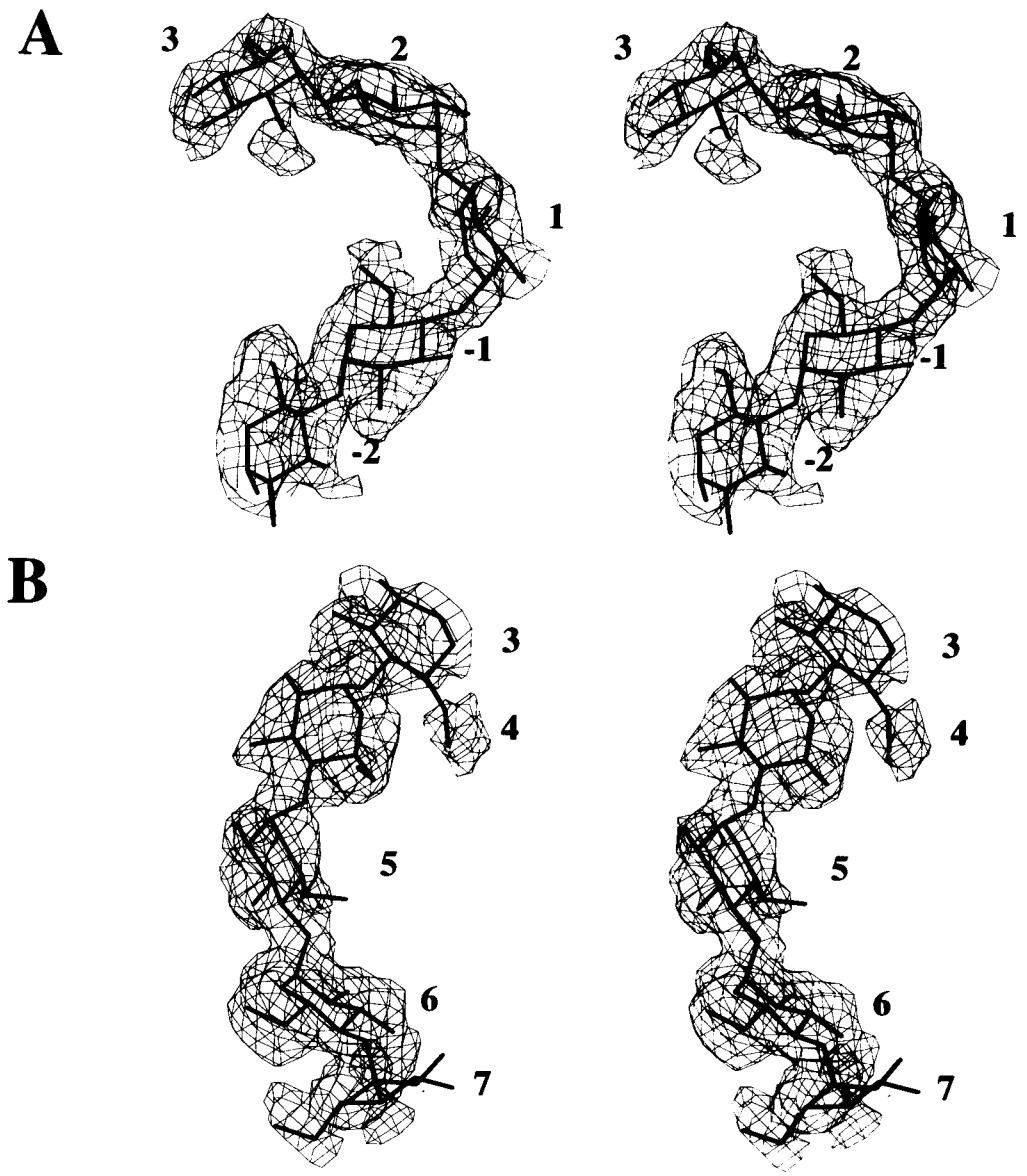

FIGURE 1: Stereoviews of a simulated annealing $2F_o - F_c$ omit map contoured at 0.6σ: (A) subsites -2 to $+3$; (B) subsites 3−7. In the nomenclature employed in this figure residues numbered 2, 1, −1, and −2 correspond to residues A, B, C, and D, respectively, of acarbose complexed to CGTase as described in Strokopytov et al. (1995).

described previously (Strokopytov et al., 1995). Residues −2, −1, and 1 all have a full $^4C_1$ chair conformation, with average temperature factors of 18.7, 11.8, 20.8, and 29.3 Å^2 for the −2, −1, 1, and 2 residues, respectively. In the complex of acarbose and CGTase the corresponding average temperature factors were 27.0, 17.3, 13.8, and 22.5 Å^2 (Strokopytov et al., 1995). The most characteristic feature of acarbose bound to CGTase is a sharp turn around the scissile glycosidic bond between subsites −1 and 1. The same conformation is observed in the complex with the maltononaose inhibitor. Since the protein−inhibitor interactions at the first four subsites near the catalytic residues have already been described in detail (Strokopytov et al., 1995), we focus in the following paragraphs on the description of the interactions of the last five sugar residues at subsites 3 through 7. Table 2 lists the observed hydrogen bonds between CGTase and residues 3−7 of the maltononaose inhibitor. In Figure 4 the overall binding mode of the maltononaose inhibitor is depicted.

Subsites 3 and 4. The sugar residue at subsite 3 has a full $^4C_1$ chair conformation and is loosely positioned between the two aromatic rings of Tyr89 and Phe195. Tyr89 is located in a flexible loop (residues 86−95) which retains the conformation observed in the uncomplexed protein. Phe195 interacts with the inhibitor rather weakly and its side chain conformation deviates little from the conformation of Tyr195 in the native structure. The protein backbone at this residue, however, has moved by about 0.8 Å toward the bound carbohydrate, and the average *B*-factor for this residue (14 Å^2) has decreased considerably from that in the uncomplexed Y195F mutant CGTase structure (39.3 Å^2) (Penninga et al., 1995), indicating that binding of the inhibitor has stabilized the protein. This is also reflected in the average overall *B*-factor of the whole protein, which has dropped from 23.3 to 13.6 Å^2.

The oligosaccharide chain at subsite 3 makes a sharp turn with respect to the preceding valienamine sugar at subsite 2 (cf. Figure 4), and as a consequence, the hydrogen bond between the O3(2) and O2(3) hydroxyl groups is lost. The intramolecular hydrogen bond between the hydroxyl groups of the glucose units at subsites 3 and 4 still exists with an O3(3)−O2(4) distance of 2.7 Å. The sugar at subsite 3 forms

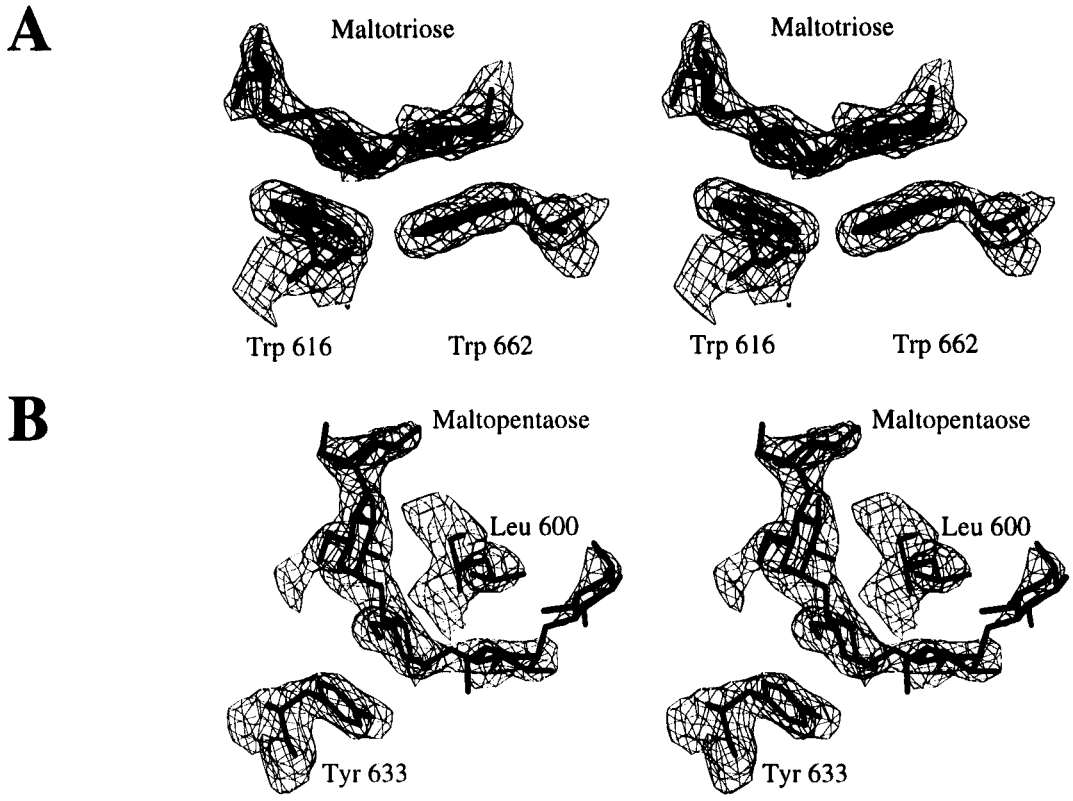

FIGURE 2: σ_a-weighted $2F_o - F_c$ electron density contoured at 1σ of (A) maltotriose bound at maltose binding site 1 and (B) maltopentaose bound at maltose binding site 2.

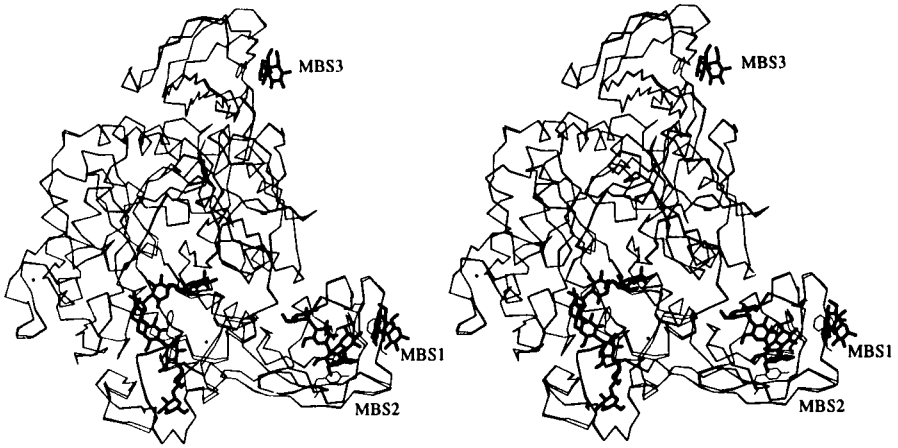

FIGURE 3: Comparison of the C_α-backbone traces of unliganded CGTase and the enzyme complexed with a maltononaose inhibitor. The largest differences in the protein backbone conformation occur in loop regions near oligosaccharide binding regions.

two hydrogen bonds with surrounding protein residues: one between the O2(3) hydroxyl group and the Asp371 side chain and one between the O6(3) hydroxyl group and the Asp196 side chain. This hydroxyl group could also interact with the O6(2) hydroxyl group which is at 2.7 Å although the geometry of this hydrogen bond is not ideal. Sugar 3 has an average *B*-factor of 33.4 Å^2.

The sugar at subsite 4 has a normal $^4C_1$ chair conformation and is only involved in internal hydrogen bonds with adjacent glucose units, involving the O3(3)−O2(4) and the O3(4)−O2(5) hydroxyl groups. It stacks loosely onto the Phe195 aromatic ring and is for a large part exposed to the solvent. Its average temperature factor is 31.3 Å^2.

Subsite 5. The sugar at subsite 5 (average *B*-factor 29.4 Å^2) has a full $^4C_1$ chair conformation as well and is involved in several water-mediated hydrogen bonds with the enzyme through its O2(5) and O3(5) hydroxyl groups. The water molecule which mediates hydrogen bonds with the main chain amino and carbonyl groups of Phe195 and Thr181, respectively, is positioned in a pocket formed by the main chain atoms of residues 193−195 and 181. In addition, a weak direct hydrogen bond between the O3(5) hydroxyl group and the main chain carbonyl oxygen of Phe195 (distance 3.1 Å) can be inferred.

Subsites 6 and 7. Both glucose residues at subsites 6 and 7 have normal $^4C_1$ chair conformations. At subsite 6 the oligosaccharide chain makes a relatively sharp turn with respect to the sugar at subsite 5. This causes the O3(5)−O2(6) hydrogen bond between the two sugars to be broken (distance 4.3 Å). The sugar at subsite 6 forms a hydrogen bond with the main chain carbonyl oxygen of Phe195 (2.7 Å) through its O2(6) hydroxyl group. The same hydroxyl

Table 2: Putative Hydrogen Bonds between CGTase and a Maltononaose Inhibitor[a]

maltononaose residue/atom	protein atom or water molecule	distance (Å)	remarks
subsite 3			
O2	Asp371 Oδ2	3.2	
O3	O2(4)	2.7	internal
O6	Asp196 Oδ1	2.7	
subsite 4			
O2	O3(3)	2.7	internal
O3	O2(5)	2.8	internal
subsite 5			
O2	O3(4)	2.8	internal
O3	water	2.7	
O3	Phe195 O	3.1	
subsite 6			
O2	Phe195 O	2.7	
O2	Asn193 Nδ2	2.9	
O3	Asn193 Nδ2	3.0	
O6	Ser455 N	3.1	symmetry-related molecule
subsite 7			
O2	Ser145 Oγ	3.4	
O2	Ser146 N	3.2	
O3	Ser145 Oγ	2.7	
O3	Asp147 N	2.8	
O4	Asp147 Oδ1	3.2	
O6	Ser455 O	3.4	symmetry-related molecule

[a] Contacts between CGTase and acarbose bound at subsites −2 through 2 have been omitted.

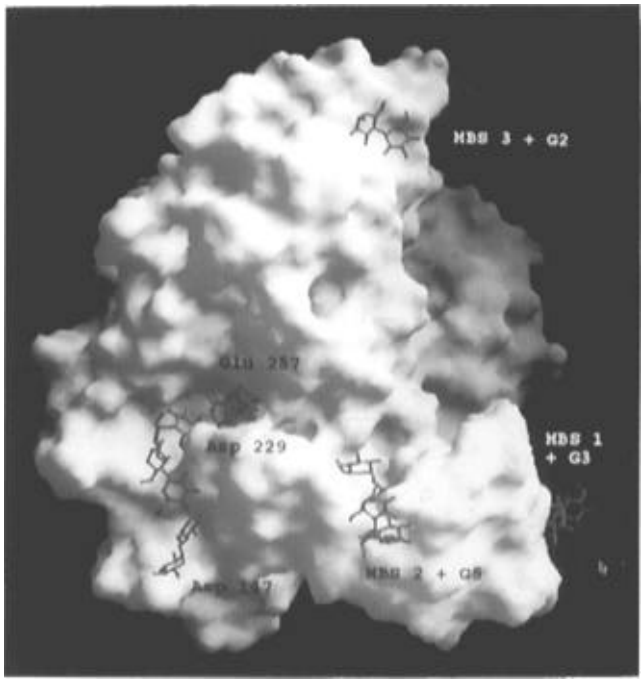

FIGURE 4: Overall binding mode of the maltononaose inhibitor and other oligosaccharides bound to CGTase from *B. circulans* strain 251, created using GRASP (Nicholls, 1992). The maltose binding sites are labeled MBS 1, MBS 2, and MBS 3. Residues important for catalysis (Asp229 and Glu257) as well as the loop region in the B domain enclosing the G9′ inhibitor (around residue 147) are indicated.

group is weakly hydrogen bonded to the side chain of Asn193. The O3(6) hydroxyl group is also involved in a hydrogen bond with the Asn193 Nδ2 group. The average temperature factors of these sugar residues are 36.6 and 42.6 Å^2, respectively.

The glucoses at subsites 6 and 7 are positioned in between two symmetry-related molecules in the crystal, thus allowing the formation of hydrogen bonds with amino acid residues of a symmetry-related molecule. The O6 hydroxyl group of the glucose at subsite 6 interacts weakly with Ser455 of a symmetry-related molecule through a hydrogen bond involving its main chain amide nitrogen (distance 3.1 Å).

The glucose residue at subsite 7 interacts with residues 145−148 which are part of a flexible loop. Upon binding of the ligand, the protein backbone of this loop moves by about 0.9 Å in order to contact the carbohydrate. This glucose residue is involved in five hydrogen bonds with surrounding protein residues. Hydrogen-bonding interactions involve the main chain amino groups of Ser146 [with O2(7)] and Asp147 [with O3(7)]. The side chain hydroxyl group of Ser145 forms a hydrogen bond with the O3(7) hydroxyl group while the Asp147 side chain interacts with the O4(7) atom, causing a slight change of conformation of Asp147 upon substrate binding. A sixth weak hydrogen bond involves residue Ser455 of a symmetry-related protein molecule and the O6(7) hydroxyl group (distance 3.4 Å). A summary of the intermolecular hydrogen-bonding interactions that can be inferred for the complex between CGTase and maltononaose is presented in Figure 5.

Binding of Carbohydrates at the Maltose Binding Sites. Analysis of the electron density near the three maltose binding sites located on the surface of the C and E domains (Lawson et al., 1994) allowed the modeling of a maltotriose at maltose binding site 1 (near Trp616 and Trp662) and a maltopentaose at maltose binding site 2 (near Tyr633). At maltose binding site 3 in the C domain (near Tyr413) only density for a maltose molecule was observed. Due to its involvement in crystal packing contacts this site is less accessible to longer oligosaccharides. Both maltopentaose and maltotriose interact with the enzyme with only two of their glucose units which replace the originally bound maltoses. No new hydrogen bonds are observed except for internal O2−O3′ hydrogen bonds.

Maltose binding site 2 lies at the bottom of a deep groove leading into the active site (Lawson et al., 1994) and could serve to guide the starch polymer into the catalytic site. The G5 molecule is slightly bent around Leu600 and directed with its nonreducing end toward the reducing end of the glucose residue at subsite −2, and the structure of the complex suggests that the maltopentaose molecule could easily be extended in order to meet with the maltononaose inhibitor. In order to span the distance between the maltopentaose bound at maltose binding site 2 and the glucose residue at subsite −2 in the active site, about four to five glucose residues are required. However, the amylose chain would be required to assume an overall twist of about 180° in this region since the C6 hydroxyl groups in the G5 and the G9 molecules are located on different sides of the polysaccharide chains. A similar turn of the oligosaccharide chain is observed for the glucose residues bound at subsites 1 and 6. Residues in the groove between the second maltose binding site and subsite −2, which may form hydrogen bonds with bound amylose, are Thr185, Glu264, and possibly Thr186 and Glu268. The hydrophobic residues Phe236, Trp258, and Tyr626 are about 7−8 Å from the bound carbohydrate but could contact it if the amylose chain would be buried deep inside the groove. The maltotriose molecule bound at maltose binding site 1 is directed with its reducing end toward the reducing end of the maltononaose inhibitor at subsite −2. This suggests that maltose binding site 1 cannot directly bind the same amylose chain as bound in

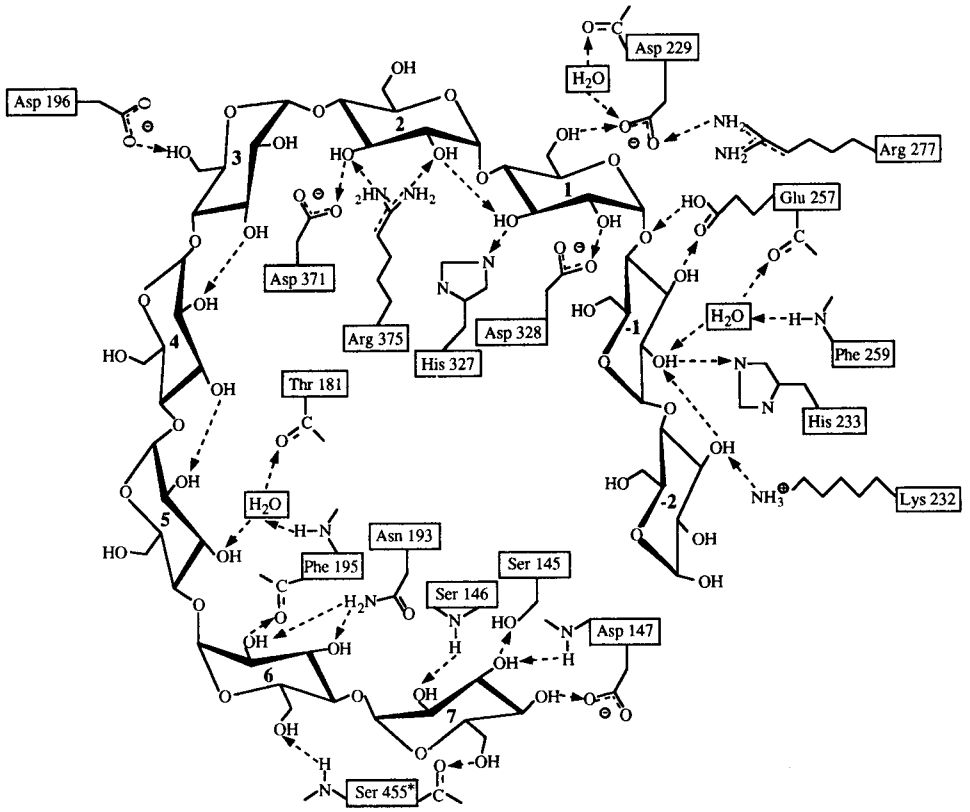

FIGURE 5: Summary of hydrogen bonds between CGTase and maltononaose bound at the active site.

the active site. Maltose binding site 2, on the other hand, could be involved in guiding the substrate into the active site.

DISCUSSION

The presence of a maltononaose inhibitor, consisting of acarbose coupled to maltopentaose, in the active site of CGTase indicates that a transglycosylation reaction involving acarbose and maltohexaose has taken place:

$$G4' + G6 \rightarrow G9' + G1 \qquad (1)$$

where the prime denotes acarbose or an acarbose-containing molecule.

Since the enzyme is expected to be inhibited by acarbose, which was added to the crystal during the first soaking step, how is the transglycosylation with maltohexaose performed? The presence of G3 and G5 bound at maltose binding sites 1 and 2, respectively, demonstrates that acarbose is capable of dissociating from the active site, yielding an active enzyme during prolonged soaking of the crystals in maltohexaose solutions. In crystals of porcine pancreatic α-amylase a seemingly similar transglycosylation reaction with acarbose has been observed (Qian et al., 1994). In that case, at pH 8, a maltose molecule was coupled to the nonreducing end of acarbose and a glucose residue was removed from the reducing end. While pancreatic amylases are capable of cleaving the reducing end glucose from acarbose (Müller et al., 1980), our CGTase from *B. circulans* strain 251 does not interconvert mixtures of G1−G4 sugars (Penninga et al., 1995) and neither acarbose nor maltotetraose is further degraded. This means that, for the coupling reaction to occur, maltohexaose has to be cleaved at the reducing end and that acarbose with its nonreducing end serves as the acceptor molecule to which G5 is coupled. This results in the G9′ compound bound in the active site. Additional evidence that G9′ is bound in the active site, rather than G9, comes from the observation that mixtures of G1−G10 sugars are good substrates for CGTase (Penninga et al., 1995). The preference for the binding of a G9′ inhibitor over oligosaccharides of a different size can be explained by the fact that the CGTase from *B. circulans* strain 251 is a *β*-CGTase with an expected preference for seven occupied subsites after the point of cleavage near Glu257.

The successful preparation of good quality crystals of CGTase complexed with the maltononaose inhibitor requires an alkaline pH. When buffer solutions of pH <9 were used for soaking with G6, cracking of the crystals was observed (data not shown). Although CGTase is still catalytically active at pH 9.8, its activity is reduced to about 30% of that at its pH optimum (Knegtel et al., 1995). Possibly such a reduction in activity allows conformational changes of the enzyme molecules in the crystal during the reaction without severe disturbance of the packing interactions. If the rate of the transglycosylation reaction is reduced, the observed increase of almost 2 Å in the length of the *c*-axis of the unit cell (Penninga et al., 1995) upon binding of oligosaccharides to the enzyme (Table 1) can more gradually be accommodated by the crystal lattice.

Although the mechanism of the hydrolysis reaction, catalyzed by CGTase, has been clarified by the structural studies of complexes between CGTase and the inhibitor acarbose (Strokopytov et al., 1995) and natural substrates (Klein et al., 1992; Knegtel et al., 1995), the mechanism by which the enzyme performs the cyclization reaction remained not well understood. Two different mechanisms have been proposed that essentially differ in the assumptions regarding the conformation of the bound amylose chain. Nakamura

et al. (1994) proposed a mechanism in which amylose binds to CGTae in a spiral conformation, while forming an inclusion complex with Tyr195, a residue that is centrally placed in the active site (Lawson et al., 1994; Penninga et al., 1995). After breaking of the glycosidic bond, the nonreducing end of the cleaved amylose chain is near its own reducing end due to the spiral conformation of the amylose chain and is subsequently coupled to the oxocarbonium intermediate that is stabilized by Asp229 at subsite 1. This scheme, however, contradicts the findings that CGTase can act on linear substrates of seven through ten glucose units, which rarely adopt a helical conformation in solution (Bender, 1990) and is not supported by the binding mode of the maltononaose inhibitor in the complex structure presented here.

The second mechanism that has been proposed assumes that the enzyme induces a curved conformation in the amylose chain (Bender, 1990; Klein et al., 1992; Strokopytov et al., 1995). This mechanism fits best with the conformation of the maltononaose inhibitor as observed in the structure of its complex with CGTase. The glucose residues at subsites 1−4 are arranged in a bent conformation, forming about one-half of a β-cyclodextrin molecule (cf. Figure 3). The glucose residues at subsites 5 through 7, however, are directed away from the active site cleft toward the loop consisting of residues 144−147 of CGTase (see Figure 4). In order for the nonreducing end of the G9 molecule to approach the oxocarbonium intermediate at subsite 1 these glucose residues would have to move past the conserved loop consisting of protein residues 179−185. The distance between the nonreducing end O4(7) oxygen of the maltononaose inhibitor at subsite 7 and the reducing end O1(1) oxygen is about 23 Å in our model. Consequently, the oxocarbonium intermediate formed after cleavage of the scissile glycosidic bond must be stabilized long enough to allow the β-cyclodextrin ring to be closed. The formation of a covalent bond between the sugar at subsite 1 and the Asp229 side chain seems an attractive possibility for such a prolonged stabilization. Although NMR studies of porcine pancreatic α-amylase in 40% DMSO at −20 °C suggested the presence of a covalently bound intermediate (Tao et al., 1989), no convincing evidence is available that in α-amylases and CGTases such a covalent intermediate is formed under physiological conditions.

The glucose residues at subsites 6 and 7 are involved in weak crystal packing contacts with symmetry-related protein molecules (cf. Table 2) which could influence the direction of the oligosaccharide chain in this region of the structure. Indeed, a sharp turn is observed at this position in the oligosaccharide chain. Several lines of evidence suggest, however, that the observed binding mode of the glucose residues bound at subsites 6 and 7 is not a crystallographic artifact. The intermolecular hydrogen bond interactions with the symmetry-related protein molecule involve only a single residue (Ser455) with donor−acceptor distances larger than 3 Å (cf. Table 2), and no hydrophobic contacts are observed. Furthermore, the observation that the second soaking with solutions containing G7, instead of G6, causes cracking of the crystals suggests that binding of the oligosaccharide chain at subsites 6 and 7 is highly specific and energetically favorable enough to distort the crystal packing. Finally, if the amylose chain bound at subsites 1−7 would bind in a more circular conformation, it would interfere with the polysaccharide chain that needs to diffuse out of the active site in order to allow for cyclization.

Our ultimate aim is to understand how the CGTase binding site should be modified in order to design a protein with high specificity toward the production of a single type of cyclodextrin. Clearly, the size of the product depends directly upon the number of glucose units which are bound in the active site before the cleavage between subsites −1 and 1 takes place. This suggests that by altering subsites in the active site it may be possible to manipulate the number of sugars which are able to bind and thus alter the ratios of α-, β-, and γ-CD produced by the enzyme. On the basis of the structure reported here, the following changes in the subsite structure for the production of increased quantities of α-, β-, or γ-CD may be proposed. In order to design an α-CGTase, the number of hydrogen bonds at subsite 6 should be increased such that preferably only six glucose units are bound to form an α-CD. In addition, a steric block could be created at subsite 7 to prevent the binding of longer oligosaccharide chains and hence the formation of larger cyclodextrins.

An enzyme that produces predominantly β-cyclodextrin should bind oligosaccharides only at subsites 1−7. Therefore, it should have the largest binding energy at subsite 7. In addition, a steric block could be introduced directly following subsite 7 in order to reduce γ-CD production. Binding up to subsite 6 should be diminished by reducing the affinity for these subsites. For instance, a number of the hydrogen bonds from subsites prior to subsite 7 could be removed by mutagenesis of the involved residues. When designing a γ-CGTase, it would be desirable to reduce the number of intermolecular hydrogen bonds before subsite 8, and again a steric block could be introduced beyond this subsite. There is no direct structural information about the conformation and position of the glucose unit at subsite 8. Model building, however, suggests that it may interact with the side chains of Ser145, Asp147, and Gln148.

In conclusion, our results suggest that subsites 6, 7, and 8 are key sites for the specificity of CGTase. Mutagenesis experiments on the amino acids involved in substrate binding at these subsites, which are likely to influence CGTase product specificity, are currently being performed.

ACKNOWLEDGMENT

We thank Dr. J. H. Branolte (Bayer Nederland, B.V.) for a gift of acarbose.

REFERENCES

Bender, H. (1990) *Carbohydr. Res. 206*, 257−267.
Bernstein, F. C., Koetzle, T. F., Williams, G. J. B., Meyer, E. F., Jr., Brice, M. D., Rodgers, J. R., Kennard, O., Shimanouchi, T., & Tasumi, M. (1977) *J. Mol. Biol. 112*, 535−542.
Brünger, A. T. (1993) *Acta Crystallogr. D49*, 24−36.
Brünger, A. T., Krukowski, A., & Erickson, J. W. (1990) *Acta Crystallogr. A46*, 585−593.
Buisson, G., Duée, E., Haser, R., & Payan, F. (1987) *EMBO J. 6*, 3909−3916.
Cheetham, J. C., Artymiuk, P. J., & Philips, D. C. (1992) *J. Mol. Biol. 224*, 613−618.
Engh, R. A., & Huber, R. (1991) *Acta Crystallogr. A47*, 392−400.
Jones, T. A. (1978) *J. Appl. Crystallogr. 11*, 268−272.
Jones, T. A., Zou, J. Y., Cowan, S. W., & Kjeldgaard, M. (1991) *Acta Crystallogr. A47*, 110−119.
Kabsch, W. (1988) *J. Appl. Crystallogr. 21*, 916−924.

Klein, C., & Schulz, G. E. (1991) *J. Mol. Biol. 217*, 737−750.
Klein, C., Hollender, J., Bender, H., & Schulz, G. E. (1992) *Biochemistry 31*, 8740−8746.
Knegtel, R. M. A., Strokopytov, B., Penninga, D., Faber, O. G., Rozeboom, H. J., Kalk, K. H., Dijkhuizen, L., & Dijkstra, B. W. (1995) *J. Biol. Chem. 270*, 29256−29264.
Larson, S. B., Greenwood, A., Cascio, D., Day, J., & McPherson, A. (1994) *J. Mol. Biol. 235*, 1560−1584.
Laskowski, R. A., MacArthur, M. W., Moss, D. S., & Thornton, J. M. (1993) *J. Appl. Crystallogr. 26*, 283−291.
Lawson, C. L., Bergsma, J., Bruinenberg, P. M., de Vries, G., Dijkhuizen, L., & Dijkstra, B. W. (1990) *J. Mol. Biol. 214*, 807−809.
Lawson, C. L., van Montfort, R., Strokopytov, B., Rozeboom, H. J., Kalk, K. H., de Vries, G., Penninga, D., Dijkhuizen, L., & Dijkstra, B. W. (1994) *J. Mol. Biol. 236*, 590−600.
Maenaka, K., Matsushima, M., Song, H., Sunada, F., Watanabe, K., & Kumagai, I. (1995) *J. Mol. Biol. 247*, 281−293.
Mattsson, P., Battchikova, N., Sippola, K., & Korpela, T. (1995) *Biochim. Biophys. Acta 1247*, 97−103.
Messerschmidt, A., & Pflugrath, J. W. (1987) *J. Appl. Crystallogr. 20*, 306−315.
Müller, L., Junge, B., & Frommer, W. (1980) in *Enzyme inhibitors* (Brodbeck, U., Ed.) pp 109−122, Verlag Chemie, Weinheim.
Nakamura, A., Haga, K., & Yamane, K. (1994) *Biochemistry 33*, 9929−9936.
Nicholls, A. (1992) *GRASP: Graphical Representation and Analysis of Surface Properties*, Columbia University, New York.
Penninga, D., Strokopytov, B., Rozeboom, H. J., Lawson, C. L., Dijkstra, B. W., Bergsma, J., & Dijkhuizen, L. (1995) *Biochemistry 34*, 3368−3376.
Qian, M., Haser, R., & Payan, F. (1993) *J. Mol. Biol. 231*, 785−799.
Qian, M., Haser, R., Buisson, G., Duée, E., & Payan, F. (1994) *Biochemistry 33*, 6284−6294.
Read, R. J. (1986) *Acta Crystallogr. A42*, 140−149.
Strokopytov, B., Penninga, D., Rozeboom, H. J., Kalk, K. H., Dijkhuizen, L., & Dijkstra, B. W. (1995) *Biochemistry 34*, 2234−2240.
Strynadka, N. C. J., & James, M. N. G. (1991) *J. Mol. Biol. 220*, 401−424.
Svensson, B., Jespersen, H. M., Sierks, M. R., & MacGregor, E. A. (1989) *Biochem. J. 264*, 309−311.
Tao, B. Y., Reilly, P. J., & Robyt, J. F. (1989) *Biochim. Biophys. Acta 995*, 214−220.
Tronrud, D. E., Ten Eyck, L., & Matthews, B. W. (1987) *Acta Crystallogr. A43*, 489−501.

BI952339H